Study of Several Potentials as Scalar Field Dark Matter Candidates

Tonatiuh Matos*, Alberto Vázquez-González* and Juan Magaña†

*Departamento de Física, Centro de Investigación y de Estudios Avanzados del IPN, A.P. 14-740, 07000 México D.F., México.
†Instituto de Astronomía, Universidad Nacional Autónoma de México, AP 70-543, 04510 D.F., México

Abstract. In this work we study several scalar field potentials as a plausible candidate to be the dark matter in the universe. The main idea is the following; if the scalar field is an ultralight boson particle, it condensates like a Bose-Einstein system at very early times and forms the basic structure of the Universe. Real scalar fields collapse in equilibrium configurations which oscillate in space-time (oscillatons). The cosmological behavior of the field equations are solved using the dynamical system formalism. We use the current cosmological parameters as constraints for the free parameters of the scalar field potentials. We are able to reproduce very well the cosmological predictions of the standard ΛCDM model with some scalar field potentials. Therefore, scalar field dark matter seems to be a good alternative to be the nature of the dark matter of the universe.

Keywords: Dark Matter, Scalar Field
PACS: 98.80.-k,95.35.+d

INTRODUCTION

Scalar fields are one of the most interesting and most mysterious fields in theoretical physics. Fundamental scalar fields are needed in all unification's theories, however, there are not experimental evidence of its existence. From the standard model of particles which needs the Higgs boson, until the superstring theory which contains the dilaton, passing through the Kaluza-Klein and the Brans-Dicke theories or thought the inflationary model, scalar fields are necessary fields. Doubtless, if they exist, they have some features which make them very special.

The *Scalar Field Dark Matter* (SFDM) model has been constructed step by step. One of the first candidates to be scalar field dark matter is the axion, one of the solutions to the strong-CP problem in QCD (see an excellent review in [21]). Essentially, the axion is a scalar field with mass restricted by observations to $\sim 10^{-5}$eV, which has its origin at 10^{-30} seconds after the big bang, when the energy of the Universe was 10^{12}GeV. This candidate is till now one of the most accepted candidates for the nature of dark matter, if its abundance is about 10^9 particles per cubic centimeter.

At the end of the last century Peebles & Vilenkin [38] proposed that a scalar field driven by inflation can behave as a perfect fluid and can have interesting observational consequences in structure formation. Besides that, they performed a sound waves analysis of this hypothesis giving some qualitative ideas for the evolution of these fields and called it fluid dark matter [39, 40]. At the same time, independently and in an opposite way, Matos & Guzmán [27] proposed that a scalar field coming from some unify the-

CP1083, *Gravitation and Cosmology, Proceedings of the Third International Meeting*
edited by F. S. Guzmán Murillo, A. Herrera-Aguilar, U. Nucamendi, and I. Quiros

ory can condensate and collapse to form halos of galaxies. Very early, this scalar field behaves as a perfect fluid, however its ultralight mass causes that the bosons condensate at very high temperature and collapse in a very different way as the fluid dark matter of Peebles & Vilenkin [38] did. They were able to fit reasonably rotation curves of some galaxies using an exact solution of the Einstein equations with an exponential potential [27, 12, 5]. The first cosmological study of the SFDM was performed in Matos & Ureña-López [30, 31] where a cosh scalar field potential was used. The cosmology reproduces all features of the Λ Cold Dark Matter (ΛCDM) model in the linear regime of perturbations.

On the other hand, Lesgourgues, Arbey & Salati [23] and Arbey, Lesgourgues & Salati [2] used a complex scalar field with a quartic potential $m^2\phi\phi^\dagger + \lambda(\phi\phi^\dagger)^2$ and solved perturbations equations (weak field limit approximation) to fit the rotational curves of dwarf galaxies with a very good accuracy, provided that $m^4/\lambda \sim 50 - 75$ eV^4. The importance of scalar fields in the dark sector has been increased, for instance, several authors have investigated the unification of dark matter and dark energy in a single scalar field [37, 2, 6]. Recently Liddle & Ureña-López [24], Liddle, Cédric & Ureña-López [25] proposed that the landscape of superstring theory can provide the Universe with a $\phi^2 + \Lambda$ scalar field potential. Such scalar field can inflate the Universe during its early epoch, after that, the scalar field can decay into dark matter. The constant Λ can be interpreted as the cosmological one. This model could explain all unknown components of the Universe in a simple way. Another interesting model in order to explain the scalar fields unification, dark sector and inflation, is using a complex scalar field protected by an internal symmetry [41].

In the present work the main idea is that if scalar fields are fundamental, they live as unified fields in some very early moment at the origin of the Universe. As the Universe expands, the scalar fields cool together with the rest of the particles until they decouple from the rest of the matter. After that, only the expansion of the Universe will keep cooling the scalar fields. If the scalar field fluctuation is under the critical temperature of condensation, the object will collapse as a BEC. After inflation, primordial fluctuations cause that the scalar fields collapse and form halos of galaxies and galaxy clusters. The cooling of scalar fields continue till the fluctuation separates from the expansion of the Universe.

In this work we study the most simple models of SFDM, using a scalar field with different potentials. In section we review the statistic of a boson gas to condensate and form a BEC, focusing in the necessary features for the BEC to form a halo of a galaxy and integrate the Einstein equations with a BEC matter. In section we transform the Einstein field equations into a dynamical system, then we numerically integrate them. We give some conditions on how these field equations can give the right behavior to reproduce the Universe we observed. In section we review a simple model which propose a new mechanism to unify inflaton-phantom using a complex scalar field. Finally in section we conclude that this SFDM model could explain the dark matter of the Universe.

SELF-GRAVITATING BEC

In this section we give some general features of the gravitational collapse of the BEC, we only pretend to show a generic behavior of any self-gravitating BEC. The BEC cosmology have been studied by Fukuyama, Masahiro & Tatekawa [11] and many numerical simulations of this collapse are given in Alcubierre et al. [1], Guzmán & Ureña-López [15], Guzmán F. S. & Ureña-López, L. [16] and besides. Guzmán, F. S. & Ureña-López [13] found that a BEC in the ground state are very stable under different initial conditions. After the Bose gas condensates the gravitational force makes the gas collapse and form self-gravitating objects. Let us suppose that the halo is spherically symmetric, which could not be to far from the reality. In that case, the space-time metric reads

$$ds^2 = -e^{2\nu}dt^2 + \frac{dr^2}{1-\frac{2MG}{r}} + r^2 d\Omega^2, \tag{1}$$

where the function $\nu = \nu(r)$ is essentially the Newtonian potential and $M = M(r)$ is the mass function given by

$$\begin{aligned} M &= 4\pi \int \rho\, r^2\, dr, \\ \frac{d\nu}{dr} &= G\frac{M + 4\pi r^3\, P}{r^2\left(1-\frac{2MG}{r}\right)}. \end{aligned} \tag{2}$$

The Einstein field equations reduce to equations (2) and the Oppenheimer-Volkov equation

$$\frac{dP}{dr} = -G\frac{(P+\rho)(M+4\pi r^3\, P)}{r^2(1-\frac{2MG}{r})}. \tag{3}$$

Let us focus in the case when the gas is far from forming a black hole. In that case we suppose that $2MG << r$ and equation (3) reduces to

$$\frac{dP}{dr} = -4\pi G r\, P(P+\rho). \tag{4}$$

The equation of state can be easily obtained from the relations $PV = 2/3\,U$, N and U developed for a Bose gas in statistical mechanics and used by Matos, Vázquez & Magaña [34]. Combining all equations we obtain that

$$\begin{aligned} P &= \frac{2\pi}{m_\phi^{8/3}}\frac{g_{5/2}(z)}{g_{3/2}(z)^{5/3}}(\rho-\rho_0)^{5/3}, && (5) \\ &= \omega(\rho-\rho_0)^{5/3}, && (6) \end{aligned}$$

where ω is the constant

$$\omega \equiv \frac{2\pi}{m_\phi^{8/3}}\frac{g_{5/2}(z)}{g_{3/2}(z)^{5/3}}, \tag{7}$$

and $\rho_0 = m_\phi < n_0 > /V$ is the mean density of the particles in the ground state. Thus, the Oppenheimer-Volkov equation (3) transforms into

$$\frac{d\rho}{dr} = -\frac{12}{5}\pi G r(\rho-\rho_0)(\omega(\rho-\rho_0)^{5/3}+\rho). \tag{8}$$

This differential equation can be easily numerically solved. Nevertheless, we have two interesting limits of equation (8). First suppose that the ω constant is small such that $P << \rho$. This situation occurs for big scalar field masses $m_\phi \sim m_{Planck}$. In that case, the equation (8) contains an analytical solution given by

$$\rho(r) = \frac{\rho_0}{1-\left(1-\frac{\rho_0}{\rho(0)}\right)e^{-\frac{6}{5}\pi G\rho_0 r^2}}, \tag{9}$$

where $\rho(0)$ is the central density of the BEC. Observe that when $r \rightharpoonup \infty$, the function $\rho(r) \rightharpoonup \rho_0$. For numerical convenience we set $\rho(0) = \varepsilon\rho_0$ in the plot, being ε a constant. The function changes dramatically for different values of ε. If $\varepsilon > 1$, the density $\rho(r)$ decreases, but if $\varepsilon < 1$ the density increases. The behavior of the density is shown in Fig. 1. This means that if the central density of the BEC is bigger than the density of

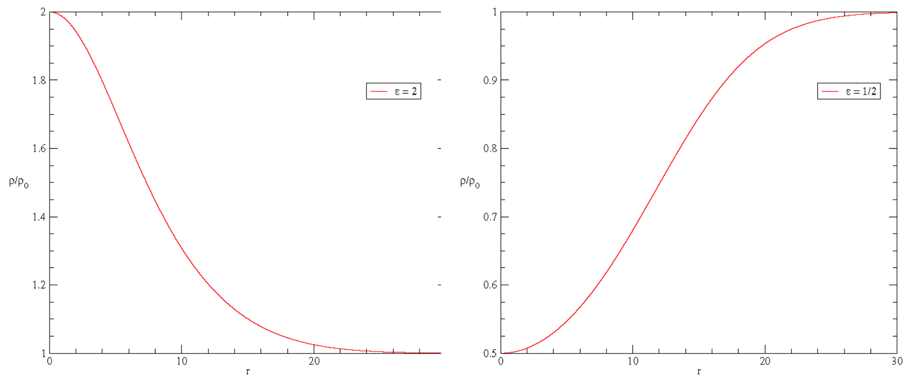

FIGURE 1. Plot of the $\rho(r)$ function given in equation (9) for $\varepsilon < 1$ (top plot) and for $\varepsilon > 1$ (down plot). The plot is done in terms of $\rho(r)/\rho_0$. We have set $\varepsilon = 2$ and $\varepsilon = 1/2$ for each plot, respectively and $\rho_0 = 0.002$.

the ground state, we have the upper profile in Fig. 1, but if it is less than it, we have the bottom profile.

The second and for us, a more interesting limit of equation (8) is when $P >> \rho$. This occurs when the scalar field mass is small enough $m_\phi << m_{Planck}$, as for astrophysical BEC. In this limit the Oppenheimer-Volkov equation has also an analytical solution given by

$$\begin{aligned}\rho(r) &= \frac{\rho(0)-\rho_0}{(2\pi G r^2\omega(\rho(0)-\rho_0)^{5/3}+1)^{3/5}}+\rho_0,\\ &= \left(\frac{p(0)/\omega}{2\pi G r^2 p(0)+1}\right)^{3/5}+\rho_0,\end{aligned} \tag{10}$$

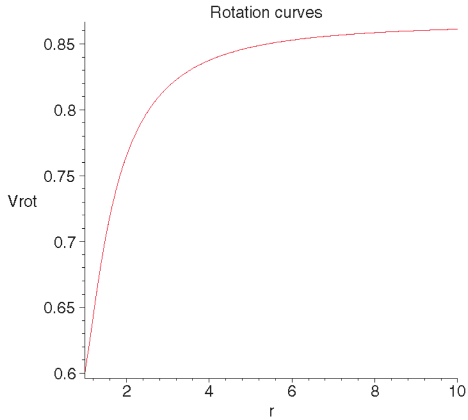

FIGURE 2. Rotation curve derived from metric (12). The velocity and the coordinate r are in arbitrary units.

or equivalently $P = 1/(2\pi G r^2 + 1/P(0))$. In this case the pressure dominates the BEC, the pressure acquire a maximum for $P(0)$. Far away enough from the center of the BEC we can approximate equation (10) with

$$\rho = \left(\frac{1/\omega}{2\pi G r^2}\right)^{3/5} + \rho_0, \tag{11}$$

which implies a space-time metric for the BEC given by

$$ds^2 = \frac{dr^2}{1 - 2(r_0 r^{4/5} + \frac{4}{3}\pi G \rho_0 r^2)} - exp(2\nu)dt^2 + r^2 d\Omega^2, \tag{12}$$

where $r_0 \equiv 10/9(4\pi^2/\omega^3)^{1/5}$. Function ν determines the circular velocity (the rotation curves) V_{rot} of test particles around the BEC. Using the geodesic equation of metric (12) one obtains that $V_{rot}^2 = r g_{tt,r}/(2g_{tt}) = r\nu'$ [29]. Using equations (2) we can integrate the function ν and obtain the rotation curves. The plot is shown in Fig. 2, where we see that the form of the rotation curves are analogous as the expected from the observed in galaxies, specially in LSB and dwarf ones [9, 10, 47] besides SFDM predicts a core density profile that could have some astrophysics advantages [44] over the standard model (cuspy profiles). However, the discussion of the central region of the rotation curves continue. This is the main reason why it is not convenient to try self-gravitating BECs in the Newtonian limit. Remain that the Newton theory can be derived from the Einstein one for slow velocities, weak fields and pressures much smaller than the densities. However these last conditions is not fulfilled in self-gravitating BEC.

From these results and from the simulations given in Guzmán, F. S. & Ureña-López [13] it follows a novel paradigm for structure formation, which is different from the bottom-up one. In the SFDM paradigm, after the big bang the scalar field expands till decouples from the rest of the matter. If the scalar field has sufficient small mass such that its critical temperature of condensation is less than the temperature of decoupling, the scalar field forms a BEC. Then the scalar field collapses forming objects which final mass is not bigger than the critical mass m^2_{Planck}/m_ϕ. These objects contain a density profile very similar to the profile shown in the top of Fig. 1. They are very stable under perturbations. It has been proposed that the dark matter in galaxies and clusters is a scalar field with a mass of 10^{-22}eV [1]. If this were the case, the main difference for the structure formation of this ultralight scalar field with the bottom-up paradigm is that the SFDM objects form just after the collapse of the scalar field and remain so during the rest of the Universe expansion. Furthermore, they can collide together but after the collision the objects remain unaltered, since they behave like solitons [4]. This means that in a merging of BEC they pass through each other without some alterations in its total mass as collision-less dark matter. This paradigm implies then that we must be able to see well formed galaxies with the actual masses for very large redshifts, longer than those predicted by the bottom-up paradigm, *i.e.*, by CDM. In this sense some authors [7] suggest a discrepancy between the observed population of massive spheroidal galaxies at high redshift with the numerical simulations of hierarchical merging in a ΛCDM scenario that under-predict this population. However, the discussion continues because other physical processes, as feedback, could have important effects in this galaxies.

THE COSMOLOGY

In this section we review the Cosmology given by a SFDM model considering several scalar field potentials as examples.

Based on the current observations of 5-year WMAP data [18] we will consider a Universe evolving in a spatially-flat Friedmann Lemaître-Robertson-Walker space-time. We assume this kind of Universe contains a real scalar field (ϕ) as dark matter, radiation (r), neutrinos (ν), baryons (b) and a cosmological constant (Λ) as dark energy.
Thus, the Lagrangian for this system is given by

$$\pounds = \sqrt{-g}\left(R - \mathscr{L}_\Phi - \mathscr{L}_\gamma\right), \tag{13}$$

where the total energy density and pressure of a homogeneous scalar field is determined by

$$\rho_\phi = \frac{1}{2}\dot{\phi}^2 + V(\phi), \;\; P_\phi = \frac{1}{2}\dot{\phi}^2 - V(\phi),$$

whereas the radiation and baryonic components are represented by perfect fluids with baryotropic equation of state $P_\gamma = (\gamma - 1)\rho_\gamma$, where γ is a constant, $0 \leq \gamma \leq 2$. For example, for radiation and neutrinos ($\gamma_{r,\nu} = \frac{4}{3}$), for baryons ($\gamma_b = 1$) and finally for a cosmological constant ($\gamma_\Lambda = 0$).

Thus, the field equations for a Universe with these components are given by

$$
\begin{aligned}
\dot{H} &= -\frac{\kappa^2}{2}(\dot{\phi}^2 + \gamma\rho_\gamma), \\
\ddot{\phi} &+ 3H\dot{\phi} + \partial_\phi V = 0, \\
\dot{\rho}_\gamma &+ 3\gamma H\rho_\gamma = 0,
\end{aligned} \tag{14}
$$

and the Friedmann equation

$$
H^2 = \frac{\kappa^2}{3}\left(\frac{1}{2}\dot{\phi}^2 + V(\phi) + \rho_\gamma\right), \tag{15}
$$

being $\kappa^2 = 8\pi G$. In order to analyze the behavior of the different components of this Universe, we are going to use the dynamical system formalism following Matos, Vázquez & Magaña [34].

Then, following the procedure for transforming equations (14) and (15), with an arbitrary potential, into a dynamical system, we define the dimensionless variables

$$
\begin{aligned}
x &\equiv \frac{\kappa}{\sqrt{6}}\frac{\dot{\phi}}{H}, \quad u \equiv \frac{\kappa}{\sqrt{3}}\frac{\sqrt{V}}{H}, \\
z_\gamma &\equiv \frac{\kappa}{\sqrt{3}}\frac{\sqrt{\rho_\gamma}}{H}.
\end{aligned} \tag{16}
$$

Using above definitions (16), the evolution equations (14) transform into an autonomous system

$$
x' = -3x + \frac{3}{2}\Pi x - \frac{\kappa}{\sqrt{6}H^2}V_{,\phi}, \tag{17a}
$$

$$
u' = \frac{3}{2}\Pi u + \frac{\kappa}{\sqrt{6}H^2}V_{,\phi}\frac{x}{u}, \tag{17b}
$$

$$
z_\gamma' = \frac{3}{2}(\Pi - \gamma)\, z_\gamma, \tag{17c}
$$

$$
-\frac{H'}{H} = \frac{3}{2}(2x^2 + \gamma z_\gamma^2) \equiv \frac{3}{2}\Pi. \tag{17d}
$$

The latter equation (17d) can be written also as

$$
s' = \frac{3}{2}\Pi s, \tag{18}
$$

for the variable $s \equiv cte/H$ and determines the evolution of the horizon. Here and in the rest of the paper, prime denotes a derivative with respect to the e-folding number $N = \ln(a)$. Moreover, the Friedmann equation (15) becomes a constraint of the variables such that

$$
F \equiv x^2 + u^2 + z_\gamma^2 = 1. \tag{19}
$$

Because we are considering an expanding Universe which implies $H > 0$ and taking into account the variable definitions (16), we can see that $u, z_\gamma \geq 0$.

On the other hand, the density rate quantities $\Omega_x = \rho_x/\rho_{crit}$ can be obtained using the variables (16), one arrives at

$$\begin{aligned} \Omega_{DM} &= x^2 + u^2, \\ \Omega_\gamma &= z_\gamma^2, \\ \Omega_\Lambda &= l^2, \end{aligned} \tag{20}$$

where we have added explicitly a cosmological constant variable $l \equiv z_\Lambda$. Besides that, with the physical constraint $0 \leq \Omega \leq 1$ and the Friedmann equation $\Omega_{DM} + \Omega_\gamma + \Omega_\Lambda = 1$ the phase space of variables $\{x, u, z_\gamma, l\}$ is bounded by

$$0 \leq x^2 + u^2 + z_\gamma^2 + l^2 \leq 1.$$

Observe that if we derive (19) with respect to N and substitute system (17) into this, we obtain

$$F' = 3\,(F-1)\,\Pi, \tag{21}$$

indicating that constraint (19) is compatible with system (17) for all scalar field potentials if the Friedmann equation is fulfilled.

Now we show that system (17) together with constraint (19) is completely integrable. To integrate system (17), first observe that we can substitute $3/2\Pi$ from equation (18) into the rest of the equations. With this substitution equation (17c) can be integrated in terms of s as

$$z_\gamma = \sqrt{\Omega_\gamma^{(0)}}\, s \exp(-\frac{3}{2}\gamma N), \tag{22}$$

where $\Omega_\gamma^{(0)}$ is an integration constant. Then we multiply (17a) by $2x$ and (17b) by $2u$ and sum both equations. We obtain

$$(x^2 + u^2)' = -6x^2 + 2\,\ln(s)'(x^2 + u^2). \tag{23}$$

After that we use constraint (19) and equation (22) into equation (23) to obtain

$$6x^2 = 2\,\ln(s)' - 3\gamma s^2\,\Omega_\gamma^{(0)} \exp(-3\,\gamma N). \tag{24}$$

Finally we have to integrate equation (18) with all these results. If we substitute (24) and (22) into (17d) or (18) we obtain $0 = 0$, that means s is an arbitrary variable which parametrizes the decrease of H and can be cast into the system as a control variable, a similar result is found by Ureña-López & Reyes-Ibarra [52]. In other words, equations (17d) and (18) are actually identities, and not equations. In what follows we will use this important result.

Thus, we set the variable s from system (17) as arbitrary in the equations (17a), (17b) and (17c).

Of course, to guess variable s in order to fulfill constraint (15) is not so easy. In order to avoid this problem we can consider the observed dynamics for H and model it by the following ansatz

$$H \equiv \frac{{t_0}^{n-1}}{t^n}, \tag{25}$$

because it is well-know the behavior for H at different epochs

$$H_{\rm dust} = \frac{2}{3t}, \; H_{\rm rad} = \frac{1}{2t}, \; H_\Lambda = \sqrt{\frac{\Lambda}{3}}. \tag{26}$$

There exists a restriction in the parameter n. Because we know from observations that H is a function monotonically decreasing, therefore n has to satisfy $n \geq 0$. With the ansatz (25), the dynamical equation for s reads

$$s' = (mt_0)^{\frac{1}{n}-1} n \left(\frac{1}{s}\right)^{\frac{1}{n}-2} = s_0 s^{-k}, \tag{27}$$

where we have defined $k \equiv 1/n - 2$.

Using this ansatz we can reduce till quadratures the solution of system (17). In order to do this, notice that

$$\frac{3}{2}\Pi = s_0 s^{-k-1}.$$

Now using the latter identity, equation (17c) can be integrated to give

$$z_\gamma = z_0 \left[s_0 (k+1) N + s_1\right]^{\frac{1}{k+1}} e^{-\frac{3}{2}\gamma N},$$

for each corresponding value of γ. Finally, equations (17a) and (17b) can be integrated as follows. We divide (17a) by x and (17b) by u and take the difference between both equations. We define $y = x/u$ to obtain

$$y' + 3y + q(N) y^2 = -q(N), \tag{28}$$

where function $q(N) = [s_0 (k+1) N + s_1]^{1/(k+1)}$. Equation (28) is a Riccati equation which can be reduce to a Bernoulli equation by defining $y = w + y_1$, where y_1 is a known solution of (28). It reduces to

$$w' + (3 + 2 q y_1) w + q z^2 = 0. \tag{29}$$

Equation (29) can be further reduced by defining $W = 1/w$, we obtain

$$W' - (3 + 2 q y_1) W - q = 0, \tag{30}$$

which its integral is

$$W = e^A \int e^{-A} q \, dN, \tag{31}$$

with $A=\int(3+2qy_1)\,dN$. Thus

$$\begin{aligned}
u &= u_0 q \exp\left(\int yq\,dN\right),\\
x &= x_0 q e^{-3N}\exp\left(-\int \frac{q}{y}\,dN\right),\\
z_\gamma &= z_0 q e^{-\frac{3}{2}\gamma N},\\
y &= \frac{1}{W}+y_1.
\end{aligned} \tag{32}$$

In the particular case where $s_0=0$, the integrals can be solved analytically, however this value for s_0 does not have any physical meaning.

On the other hand, we can evaluate the integrals using numerical methods for different values of the free constants. We can obtain a numerical solution for the system using () or directly integrating system (17) with an Adams-Bashforth-Moulton (ABM) method and using as initial data the WMAP+BAO+SN recommended values to $\Omega_\Lambda^{(0)}=0.721$, $\Omega_{DM}^{(0)}=0.233$, $\Omega_b^{(0)}=0.0454$, $\Omega_r^{(0)}=0.0004$, $\Omega_\nu^{(0)}=0.0002$, the result is the same.

For a more general study about the solutions′ stability see Matos, Vázquez & Magaña [34]

The ϕ^2 scalar potential

We start our cosmological analysis of SFDM taking the potential

$$V(\phi)=\frac{1}{2}m^2\phi^2, \tag{33}$$

developing the standard procedure to transform it into a dynamical system. Using the definitions given in (16), the evolution equations (14) for potential (33) transform into an autonomous system

In the following, we investigate if this system can reproduce the observed Universe. We introduce the components of the background Universe into the dynamical system described by (17) adding to it baryons (b), radiation (z) and neutrinos (ν). Thus, the system transforms into

$$
\begin{aligned}
x' &= -3x - su + \frac{3}{2}\Pi x, && \text{(34a)}\\
u' &= sx + \frac{3}{2}\Pi u, && \text{(34b)}\\
b' &= \frac{3}{2}\left(\Pi - 1\right) b, && \text{(34c)}\\
z' &= \frac{3}{2}\left(\Pi - \frac{4}{3}\right) z, && \text{(34d)}\\
v' &= \frac{3}{2}\left(\Pi - \frac{4}{3}\right) v, && \text{(34e)}\\
l' &= \frac{3}{2}\Pi l, && \text{(34f)}\\
s' &= s_0 s^{-k}, && \text{(34g)}
\end{aligned}
$$

with $\Pi = 2x^2 + b^2 + \frac{4}{3}z^2 + \frac{4}{3}v^2$ and the Friedman equation reduces to the constraint

$$
F = x^2 + u^2 + b^2 + z^2 + v^2 + l^2 = 1. \tag{35}
$$

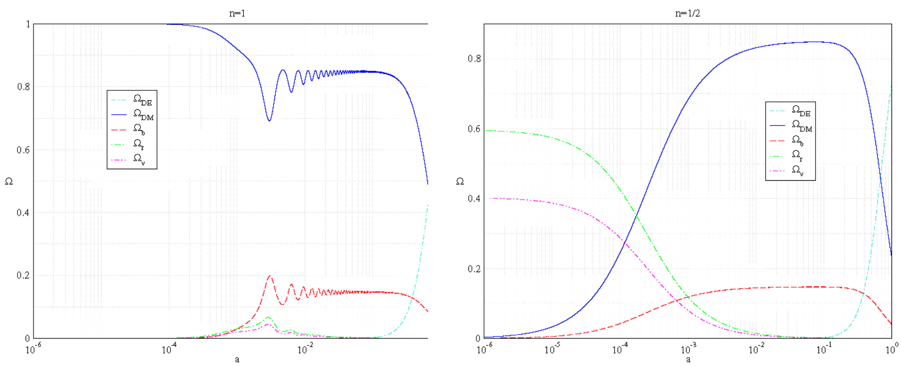

FIGURE 3. Evolution of the density parameters for the system (34) with $n = 2$ (top panel) This values of n are not reproduce the standard behavior of ΛCDM and $n = 1/2$ SFDM reproduces the standard ΛCDM behavior (bottom panel).

Figure 3 shows the numerical solutions of the dynamical system (34). In Fig. 3 we have set $n = 2, 1/2$ as examples. From these figures it is clear that for $n = 2$ and some other values such that $n \geq 1$ the radiation remains sub-dominant. It means, these values of n are not able to explain the big bang nucleosynthesis, since radiation never dominates as it is required. On the other hand, where the plot is made for $n = 1/2$, and for $0 \geq n > 1$, the radiation and the neutrinos behave exactly in the same way as they do in the ΛCDM model, so we expect that these can reproduce the observed Universe. Following the radiation dominated era, ϕ^2 dark matter becomes the component that dominates the evolution and finally the Universe is dominated by the cosmological constant. Figure 4

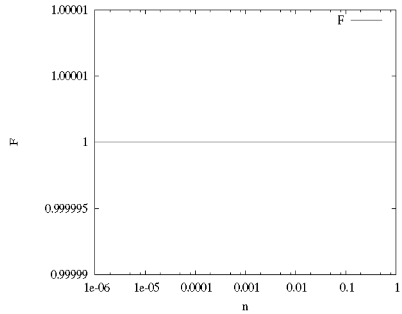

FIGURE 4. Evolution of the function $F = x^2 + u^2 + b^2 + z^2 + v^2 + l^2$ in (35) for the system (34) with $n = 1, 5, 1/2$ and $1/5$. Function F is exactly the same for all values of n in all these cases.

shows the constraint F in (35) in order to visualize the integration's error. Observe that $F \approx 1$ at every point in the evolution, indicating that the Friedmann equation is exactly fulfilled all the time, this behavior is exactly the same for all runs.

The *cosh* scalar potential

Now, we are going to compare the above results with the potential

$$V(\phi) = V_0 \left[\cosh(\kappa\lambda\phi) - 1\right]. \tag{36}$$

where v_0 and λ are free parameters. In order to do so, we introduce new couple of variables

$$\begin{aligned} u &\equiv \sqrt{\frac{2V_0}{3}}\frac{\kappa}{H}\cosh\left(\frac{1}{2}\kappa\lambda\phi\right), \\ v &\equiv \sqrt{\frac{2V_0}{3}}\frac{\kappa}{H}\sinh\left(\frac{1}{2}\kappa\lambda\phi\right). \end{aligned} \tag{37}$$

Substituting definitions (37) and (16) into equations (14) we obtain

$$\begin{aligned} x' &= -3x - \lambda v u + \frac{3}{2}\Pi x, \\ u' &= \lambda x v + \frac{3}{2}\Pi u, \\ v' &= \lambda x u + \frac{3}{2}\Pi v, \\ z_\gamma' &= \frac{3}{2}(\Pi - \gamma)\, z_\gamma, \\ l' &= \frac{3}{2}\Pi l, \end{aligned} \tag{38}$$

where we are also using the function $\Pi = 2x^2 + \gamma z^2$. Besides that, from the definitions (37) it follows the constraint

$$u^2 - v^2 = \frac{2V_0\,\kappa^2}{3}\frac{1}{H^2} = \frac{1}{\lambda^2}\frac{m_\phi^2}{H^2}, \tag{39}$$

and the Friedmann equation (15) written in these variables reads

$$F = x^2 + u^2 + z_\gamma^2 + l^2 = 1. \tag{40}$$

However, equation (40) is actually not real constraint, since they are inhered in the dynamical equations (38) (see the above section). Furthermore, constraint (39) is also inhered in the dynamical system, observe that if we multiply the second equation of (38) by $1/2u$ and the third by $1/2v$ and rest each other, we obtain

$$H' = -\frac{3}{2}\Pi H. \tag{41}$$

But this relation follows directly from the field equations (14). This means that system (38) is compatible with the constraint (39). Using this constraint (39) in the dynamical system (38), we obtain

$$\begin{aligned}
x' &= -3x - u\sqrt{\lambda^2 u^2 + \left(\frac{m}{H}\right)^2} + \frac{3}{2}\Pi x,\\
u' &= x\sqrt{\lambda^2 u^2 + \left(\frac{m}{H}\right)^2} + \frac{3}{2}\Pi u,\\
z' &= \frac{3}{2}\left(\Pi - \gamma\right) z,\\
l' &= \frac{3}{2}\Pi l.
\end{aligned} \tag{42}$$

We notice, that occurs the same situation as ϕ^2 potential. Introducing again the variable $s \equiv cte/H$ with its dynamical equation.

$$s' = s_0 s^{-k} \tag{43}$$

we obtain

$$\begin{aligned}
x' &= -3x - u\sqrt{\lambda^2 u^2 + s^2} + \frac{3}{2}\Pi x,\\
u' &= x\sqrt{\lambda^2 u^2 + s^2} + \frac{3}{2}\Pi u,\\
z_\gamma' &= \frac{3}{2}\left(\Pi - \gamma\right) z_\gamma,\\
l' &= \frac{3}{2}\Pi l,\\
s' &= s_0\, s^{-k}.
\end{aligned} \tag{44}$$

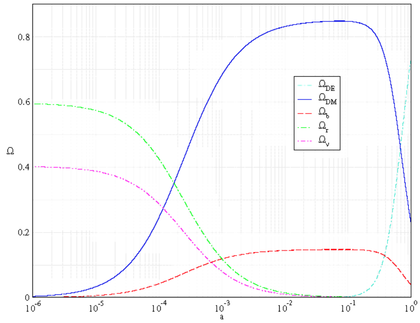

FIGURE 5. Evolution of the density parameters for the system (44), where the scalar field potential is given by the equation (36).

The density parameters are the same as we have defined at (20). We solve numerically (44) with the same initial conditions as the system of equations (34) and $\lambda \approx 20$ Matos, et.al. [35]. The solution is shown in Fig. (5). The plot shows the dynamical evolution for a Universe with SFDM with the potential (36), notice that is equivalent to potential (33).

The ϕ^3 scalar potential

Now, we analyze the cubic potential

$$V(\phi) = \frac{1}{3}\phi^3, \tag{45}$$

With this potential, variable u reads

$$u \equiv \frac{\kappa}{3H}\phi^{3/2}, \tag{46}$$

Substituting definition (46) and (16) into equations (14) we obtain

$$\begin{aligned} x' &= -3x - \lambda s^{\frac{2}{3}} u^{\frac{4}{3}} + \frac{3}{2}\Pi x, \\ u' &= \lambda x s^{\frac{2}{3}} u^{\frac{1}{3}} + \frac{3}{2}\Pi u, \\ z'_\gamma &= \frac{3}{2}(\Pi - \gamma) z_\gamma, \\ l' &= \frac{3}{2}\Pi l, \end{aligned} \tag{47}$$

where $\lambda \equiv 3^{5/6}/\sqrt{2}$. Again, we have introduced an external variable $s \equiv 1/H$ as a control variable for the dynamics of H with its dynamical equation

$$s' = s_0 s^{-k}, \tag{48}$$

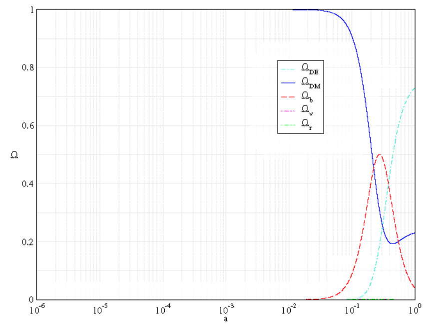

FIGURE 6. Evolution of the density parameters for the system (49), where the scalar field potential is given by the equation (45).

where s_0 is a constant. The Friedmann equation is the same as (40).

From previous sections, we have seen that this constraint is implicit in the dynamical system (47).

Finally, we obtain the close dynamical system for the scalar potential (45)

$$x' = -3x - \lambda s^{\frac{2}{3}} u^{\frac{4}{3}} + \frac{3}{2}\Pi x, \tag{49a}$$

$$u' = \lambda x s^{\frac{2}{3}} u^{\frac{1}{3}} + \frac{3}{2}\Pi u, \tag{49b}$$

$$z'_\gamma = \frac{3}{2}(\Pi - \gamma) z_\gamma, \tag{49c}$$

$$l' = \frac{3}{2}\Pi l, \tag{49d}$$

$$s' = s_0 s^{-k}, \tag{49e}$$

The density parameters are the same as we have defined at (20). We solve numerically (49) with the same initial conditions as the system of equations (34) and (44). The solution is shown in Fig. (6). The plot shows the dynamical evolution for a Universe with SFDM using the potential (45). Observe that at early times the radiation field does not dominate the Universe as required and the other fields have not the behavior predicted by the standard model. Therefore this scalar potential cannot reproduce the dynamics of the observed Universe and then is not a good candidate to be the dark matter.

The ϕ^4 scalar potential

Now, we are going to analyze the potential

$$V(\phi) = \frac{1}{4}\phi^4, \tag{50}$$

With this potential, variable u is defined as

$$u \equiv \frac{\kappa}{2\sqrt{3}}\frac{\phi^2}{H}, \tag{51}$$

Substituting definition (51) and (16) into equations (14) we obtain

$$\begin{aligned}
x' &= -3x - \lambda s^{\frac{1}{2}} u^{\frac{3}{2}} + \frac{3}{2}\Pi x, \\
u' &= \lambda x s^{\frac{1}{2}} u^{\frac{1}{2}} + \frac{3}{2}\Pi u, \\
z'_\gamma &= \frac{3}{2}(\Pi - \gamma) z_\gamma, \\
l' &= \frac{3}{2}\Pi l,
\end{aligned} \tag{52}$$

where $\lambda \equiv 3^{1/4}2$. As in the cases showed above, we must introduce the external variable $s \equiv 1/H$ as a control variable for the dynamics of H with its dynamical equation (27). Again the Friedmann equation is given by equation (40) and we do not need to solve this equation because it is implicit in the dynamical system (52). We obtain the close dynamical system for the scalar potential (50)

$$x' = -3x - \lambda s^{\frac{1}{2}} u^{\frac{3}{2}} + \frac{3}{2}\Pi x, \tag{53a}$$

$$u' = \lambda x s^{\frac{1}{2}} u^{\frac{1}{2}} + \frac{3}{2}\Pi u, \tag{53b}$$

$$z'_\gamma = \frac{3}{2}(\Pi - \gamma) z_\gamma, \tag{53c}$$

$$l' = \frac{3}{2}\Pi l, \tag{53d}$$

$$s' = s_0 s^{-k}, \tag{53e}$$

The density parameters are the same as we have defined at (20). We solve numerically (53) with the same initial conditions as the system of equations (34) and (44). The solution is shown in Fig. (7). The plot shows the dynamical evolution for a Universe with SFDM with the potential (50), observe that the behavior is exactly the same as ϕ^3 potential, therefore this potential is either a good candidate to be SFDM.

The *exp* scalar potential

Finally we analyze the exponential potential

$$V(\phi) = V_0 e^{\lambda \phi}, \tag{54}$$

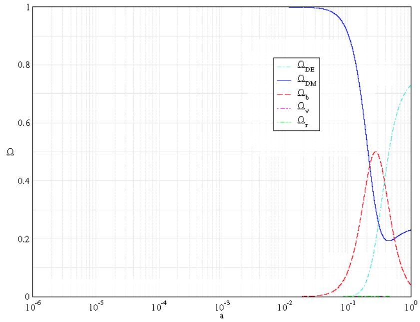

FIGURE 7. Evolution of the density parameters for the system (53), where the scalar field potential is given by the equation (50).

where V_0 and λ are free parameters. With the potential (54), variable u reads

$$u \equiv \frac{\kappa}{3}\frac{\sqrt{V_0}}{H}e^{\lambda\phi/2}, \tag{55}$$

Substituting definition (55) and (16) into equations (14) we obtain

$$\begin{aligned} x' &= -3x - \hat{\lambda}u^2 + \frac{3}{2}\Pi x, \\ u' &= \hat{\lambda}xu + \frac{3}{2}\Pi u, \\ z_\gamma' &= \frac{3}{2}(\Pi - \gamma)\, z_\gamma, \\ l' &= \frac{3}{2}\Pi l, \end{aligned} \tag{56}$$

where $\hat{\lambda} \equiv \sqrt{3}\lambda/\sqrt{2}k^2$. In this case, the system is completely autonomous and is not necessary to introduce a external control parameter s for the Hubble parameter H. Thus, the Friedmann equation (15) written in these variables reads

$$F = x^2 + u^2 + z_\gamma^2 + l^2 = 1. \tag{57}$$

The above equation is only used in order to compute the integration's error for our numerical method.

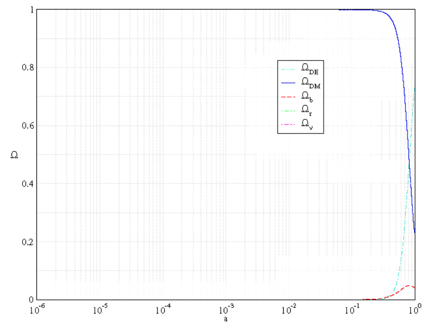

FIGURE 8. Evolution of the density parameters for the system (58), where the scalar field potential is given by the equation (54).

Thus the whole close system is given by

$$x' = -3x - \lambda u^2 + \frac{3}{2}\Pi x, \tag{58a}$$

$$u' = \lambda x u + \frac{3}{2}\Pi u, \tag{58b}$$

$$z'_\gamma = \frac{3}{2}(\Pi - \gamma)\, z_\gamma, \tag{58c}$$

$$l' = \frac{3}{2}\Pi l, \tag{58d}$$

$$s' = s_0 s^{-k}, \tag{58e}$$

The density parameters are the same as we have defined in (20). We solve numerically (58) with the same initial conditions as the system of equations (34), (44) and (49) and $\hat{\lambda} > 0$. The solution is shown in Figure (8). The plot shows the dynamical evolution for a Universe with SFDM with the potential (54), notice that the behavior of this Universe is not in agreement with the predictions of the standard model, therefore we can rule out this potential as a possible candidate to dark matter.

It is remarkable that the dynamic of ϕ^2 and *cosh* scalar field potentials are indistinguishable from the cold dark matter standard model. Thus they can be proposed as an alternative candidates to the nature of dark matter. Unfortunately, all the other potentials can be ruled out because they can not reproduce the observed dynamic of our Universe.

SCALAR FIELDS UNIFICATION

In Pérez-Lorenzana, Montesinos & Matos [41] it was proposed a new mechanism to unify scalar fields in order to have inflation and late accelerating expansion of the Universe, using a complex scalar field (inflaton-phantom unification) protected by an internal $SO(1,1)$ symmetry. In this work the authors analyze the corresponding cosmology and the stability of the fields. They consider the Lagrange density

$$\pounds = \sqrt{-g}\left(R - \mathscr{L}_\Phi - \mathscr{L}^*_\Phi - \mathscr{L}_\gamma\right),$$

where $\mathscr{L} = \frac{1}{2}\partial^\sigma\Phi\partial_\sigma\Phi + V$ is the scalar field Lagrangian endowed with the scalar field potential V. In this way, the scalar field Lagrangian in terms of the real scalar field contains the inflaton part φ_1 and the phantom part φ_2

$$\mathscr{L}_\Phi + \mathscr{L}^*_\Phi = \frac{1}{2}\partial^\sigma\varphi_1\partial_\sigma\varphi_1 - \frac{1}{2}\partial^\sigma\varphi_2\partial_\sigma\varphi_2 + 2V$$

In an homogeneous and isotropic universe, the field equations can be written as

$$\begin{aligned} \Box\varphi_1 - \frac{\partial V}{\partial\varphi_1} &= 0, \\ \Box\varphi_2 + \frac{\partial V}{\partial\varphi_2} &= 0, \\ \dot\rho_\gamma + 3H\gamma\rho_\gamma &= 0, \end{aligned} \tag{59}$$

where for simplicity we have set

$$V = V(\varphi_1, \varphi_2)$$

and $\Box = 1/\sqrt{-g}\partial_\mu(\sqrt{-g}g^{\mu\nu}\partial_\nu)$ is the D'Alambertian in the Friedman-Robertson-Walker (FRW) space-time

$$ds^2 = -dt^2 + a^2\left[\frac{dr^2}{1-kr^2} + r^2(d\theta^2 + \sin^2(\theta)d\varphi^2)\right]$$

With these definitions, the field equations of the system are the Friedmann equation

$$H^2 + \frac{k}{a^2} = \frac{\kappa}{3}\left(\frac{1}{2}\dot\varphi_1{}^2 - \frac{1}{2}\dot\varphi_2{}^2 + V(\varphi_1,\varphi_2) + \rho_\gamma\right) \tag{60}$$

and the corresponding Klein-Gordon equations for the fields φ_1 and φ_2

$$\begin{aligned} \ddot\varphi_1 + 3H\dot\varphi_1 + \frac{\partial V}{\partial\varphi_1} &= 0, \\ \ddot\varphi_2 + 3H\dot\varphi_2 - \frac{\partial V}{\partial\varphi_2} &= 0, \\ \dot\rho_\gamma + 3H\gamma\rho_\gamma &= 0, \end{aligned} \tag{61}$$

where ρ_γ stands for the different perfect fluid content of the system with state equations $p_\gamma = (\gamma - 1)\rho_\gamma$. In order to study the stability and the evolution of system (61), it is convenient to define new variables dimensionless, as we did in the case of a single scalar field, these variables can be defined as

$$
\begin{aligned}
x &\equiv \frac{\sqrt{\kappa}}{\sqrt{6}}\frac{\dot{\varphi}_1}{H},\ A \equiv \frac{\sqrt{\kappa}}{\sqrt{6}}\frac{\dot{\varphi}_2}{H},\\
\xi &\equiv \frac{\sqrt{\kappa}}{\sqrt{3}}\frac{\sqrt{V}}{H},\ s \equiv \frac{1}{H},\\
z_\gamma &\equiv \frac{\sqrt{\kappa}}{\sqrt{3}}\frac{\sqrt{\rho_\gamma}}{H}
\end{aligned} \tag{62}
$$

where z_γ stands for all the perfect fluids. With these new variables the field equations (61) transform into

$$x' = -3x - U + \frac{3}{2}\Pi x, \tag{63a}$$

$$A' = -3A + W + \frac{3}{2}\Pi A, \tag{63b}$$

$$z'_\gamma = \frac{3}{2}(\Pi - \gamma) z_\gamma, \tag{63c}$$

$$l' = \frac{3}{2}\Pi l, \tag{63d}$$

$$s' = \frac{3}{2}\Pi s \tag{63e}$$

And the Friedman equation (60) transforms into the constrain

$$F = x^2 - A^2 + \xi^2 + z_\gamma^2 + l^2 = 1 \tag{64}$$

where now $\Pi = 2x^2 - 2A^2 + \gamma z_\gamma^2$ and we have defined the potentials

$$U \equiv \frac{\sqrt{\kappa}}{\sqrt{6}}\frac{1}{H^2}\frac{\partial V}{\partial \varphi_1},\ W \equiv \frac{\sqrt{\kappa}}{\sqrt{6}}\frac{1}{H^2}\frac{\partial V}{\partial \varphi_2} \tag{65}$$

Notice that this kind of analysis is developed for an arbitrary potential. Nevertheless, the whole system is not already close, due to the presence of V which depends on both variables (φ_1, φ_2). So, in order to close the system we introduce a couple of auxiliary variables which help to complete the dynamical system and its dynamical equations.

$$u \equiv \frac{\sqrt{\kappa}}{\sqrt{6}}\frac{M_1\varphi_1}{H},\ w \equiv \frac{\sqrt{\kappa}}{\sqrt{6}}\frac{M_2\varphi_2}{H} \tag{66}$$

with

$$u' \equiv M_1 x s + \frac{3}{2}\Pi u, \tag{67}$$

$$w' \equiv M_2 A s + \frac{3}{2}\Pi w, \tag{68}$$

Summarizing, giving an arbitrary potential we calculate the parameters U, W, ξ and therefore the set of equations which determines the universe evolution with two fields are described by

$$x' = -3x - U + \frac{3}{2}\Pi x, \quad (69a)$$

$$u' = M_1 x s + \frac{3}{2}\Pi u, \quad (69b)$$

$$A' = -3A + W + \frac{3}{2}\Pi A, \quad (69c)$$

$$w' = M_2 A s + \frac{3}{2}\Pi w, \quad (69d)$$

$$z'_\gamma = \frac{3}{2}(\Pi - \gamma) z_\gamma, \quad (69e)$$

$$l' = \frac{3}{2}\Pi l, \quad (69f)$$

$$s' = \frac{3}{2}\Pi s \quad (69g)$$

Observe that system (69) is compatible with (64), *i.e.*, the derivative of F with respect to N is $F' = 3\Pi(F-1)$. This means that if we start with $F = 1$, the system will remain in this value all the time, as in the single scalar field case. We will use constriction (64) as a numerical indicator of the accuracy of the results. Making a similar procedure to the single scalar field, we find that equation (69g) is actually an identity and not really an equation for s. Thus, we can chose the function s in such a way that we can integrate system (69) numerically and check the accuracy of the method using constrain (64). For example, if we use the Hubble parameter as $H \sim t^{-n}$, where t is the cosmological time, the behavior of the derivative of the parameter $s' \sim s^{-k}$, with $k = 2 - 1/n$. Hence, we will use this behavior of s' as an ansatz instead of the equation (69g) in order to integrate system (69) numerically.

In what follows we analyze some examples.

Example 1: Two Parameters Quadratic Potential

In this section we give an example using the invariants of the theory (see also Matos, et.al. [36]). Consider for instance the simple potential

$$V(\Phi) = \frac{1}{4}M_1^2\left(\Phi^T\sigma_3\Phi + \Phi^\dagger\Phi\right) - \frac{1}{2}M_2^2\Phi^\dagger\sigma_1\Phi + V_0,$$

built out of the three $SO(1,1)$ invariants. It can be written in terms of real component fields as

$$V = \frac{1}{2}M_1^2\left(\varphi_1 - \frac{M_2^2}{M_1^2}\varphi_2\right)^2 - \frac{1}{2}\frac{M_2^4}{M_1^2}\varphi_2^2 + V_0\,. \quad (70)$$

The potential is unbounded, but this should not be a matter of concern due to unusual dynamics of the phantom. Thus, for this potential we have

$$U = M_1\,u\,s - M_2\,w\,s \quad , \qquad W = -\frac{M_2^2}{M_1}u\,s.$$

$$\xi^2 \;=\; u^2 - \frac{2M_2}{M_1}u\,w \tag{71}$$

With the variables (62) equations (69) transform into a dynamical system for the variables $\{x, u, A, w, z_\gamma, l, s\}$.

$$x' = -3x - M_1\,u\,s + M_2\,w\,s + \frac{3}{2}\Pi x, \tag{72a}$$

$$u' = M_1\,s\,x + \frac{3}{2}\Pi u, \tag{72b}$$

$$A' = -3A - \frac{M_2^2}{M_1}u\,s + \frac{3}{2}\Pi A, \tag{72c}$$

$$w' = M_2\,s\,A + \frac{3}{2}\Pi w, \tag{72d}$$

$$z'_\gamma = \frac{3}{2}\,(\Pi - \gamma)\,z_\gamma, \tag{72e}$$

$$l' = \frac{3}{2}\Pi\,l, \tag{72f}$$

$$s' = s_0\,s^{-k} \tag{72g}$$

where z_γ represents the perfect fluid components, for baryons $(\gamma = 1)$ and for radiation $(\gamma = 4/3)$. The function Π is now

$$\Pi = 2x^2 - 2A^2 + \gamma z_\gamma^2. \tag{73}$$

As usual, the Friedmann equation transforms into a constriction for the dynamical system (69) given for the hyperboloid equation

$$x^2 - A^2 + z_\gamma^2 + l^2 + u^2 - \frac{2M_2}{M_1}u\,w = 1 \tag{74}$$

Notice that the variables u and w are coupled, thus the density parameters for both fields can not evolve independently. The convenience of defining the new variables (62) is evident when we write the density rates of the Universe. Let ρ_{crit} the critical density of the Universe, then, the density rates $\Omega_x = \rho_x/\rho_{crit}$ are given by

$$\Omega_{\varphi_1} + \Omega_{\varphi_2} \;=\; x^2 + u^2 - A^2 - \frac{2M_2}{M_1}u\,w$$

$$\Omega_b \;=\; z_b^2 \quad \Omega_r = z_r^2,$$

$$\Omega_\Lambda \;=\; l^2. \tag{75}$$

where Ω_b, Ω_r, Ω_Λ are respectively the baryon, radiation and the constant V_0 density rates and Ω_{φ_1} and Ω_{φ_2} are the density rates of the corresponding scalar fields. The results are showed in Figures (10) and (9)

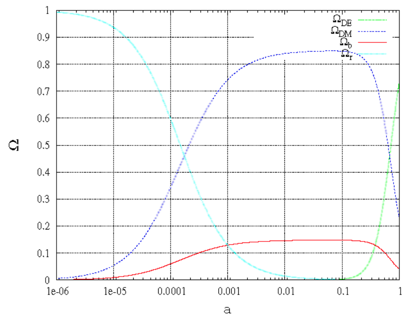

FIGURE 9. . Late Universe. We plot the evolution of the densities $\Omega_{\varphi_1} = \Omega_{DM}$, $\Omega_{\varphi_2} = \Omega_{DE}$, $\Omega_{radiation}$ and $\Omega_{baryons}$. The initial conditions we use here are the observed values from WMAP5 and SDSS. The masses are $M_1 = 1$ and $M_2 = 10^{-5}$. The integration is made using the Adams-Bashforth-Moulton (ABM) method, integrating from $a = 1$ till $a = 10^{-6}$. The initial values for $s = 1000$, $x = 10^{-2}$ and $A = 0$.

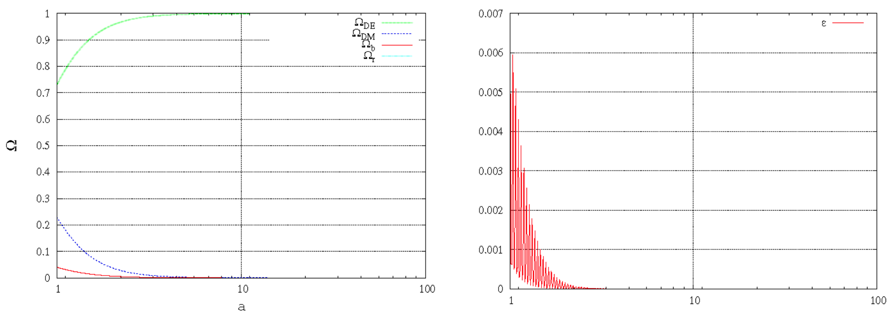

FIGURE 10. Early Universe. In these plots we show the evolutions of the fields (upper panel) during $N = 100$-folds. We see that the u field is a source while the ξ and the w fields are attractors. In the low panel we show the evolution of the slow roll parameter ε. Observe that this parameter is small after 10-folds, indicating that the system enters into a period of inflation. Here $M_2 \sim 1 \times 10^{-5} M_1$ and the densities are $u = 10^{-5}$, $w = 10^{-5}$ at $N = 1$

Example 2: Three Parameters Quadratic Potential

In this section we give an example using a more general invariant of the theory (see also Matos, et.al. [36]). Consider for instance the simple potential

$$V(\Phi) = \frac{1}{4} M_1^2 \Phi^T \sigma_3 \Phi + \frac{1}{4} M_2^2 \Phi^\dagger \Phi \pm \frac{1}{2} m^2 \Phi^\dagger \sigma_1 \Phi + V_0 \,, \tag{76}$$

built out of the three $SO(1,1)$ invariants. It can be written in terms of real component fields as

$$\begin{aligned} V &= \frac{1}{4}(M_1^2+M_2^2)\varphi_1^2+\frac{1}{4}(M_2^2-M_1^2)\varphi_2^2 \\ &\pm \frac{m^2}{2}\varphi_1\varphi_2+V_0\,. \end{aligned} \tag{77}$$

In what follows for facility we make the transformation

$$M_1^2+M_2^2 \rightarrow 2M_1^2 \tag{78}$$

$$M_1^2-M_2^2 \rightarrow 2M_2^2. \tag{79}$$

The potential as defined in (77) is now defined as

$$V=\frac{1}{2}M_1^2\varphi_1^2 \pm m^2\varphi_1\varphi_2-\frac{1}{2}M_2^2\varphi_2^2. \tag{80}$$

$$U=\frac{m^2}{M_2}sw+M_1su \quad , \qquad W=\frac{m^2}{M_1}su-M_2sw$$

$$\xi^2 = u^2-w^2+\frac{2m^2}{M_1M_2}uw \tag{81}$$

In this work we will take only the plus sign. Again we use these new variables to transform equations (60-61) into the dynamical system for the variables $\{x,u,A,w,z_\gamma,l,s\}$, given by

$$x' = -3x-\frac{m^2}{M_2}sw-M_1su+\frac{3}{2}\Pi x, \tag{82a}$$

$$u' = M_1sx+\frac{3}{2}\Pi u, \tag{82b}$$

$$A' = -3A+\frac{m^2}{M_1}su-M_2sw+\frac{3}{2}\Pi A, \tag{82c}$$

$$w' = M_2sA+\frac{3}{2}\Pi w, \tag{82d}$$

$$z_\gamma' = \frac{3}{2}(\Pi-\gamma)z_\gamma, \tag{82e}$$

$$l' = \frac{3}{2}\Pi l, \tag{82f}$$

$$s' = \frac{3}{2}\Pi s \tag{82g}$$

$$x^2-A^2+z_\gamma^2+l^2+u^2-w^2+\frac{2m^2}{M_1M_2}uw=1 \tag{83}$$

where the perfect fluid components for baryons and for radiation are represented by z_γ. The function Π is the same as equation (73), the function F is given by (74) and the rate densities are the same as in (75). The results are shown in Figures (13) and (11)

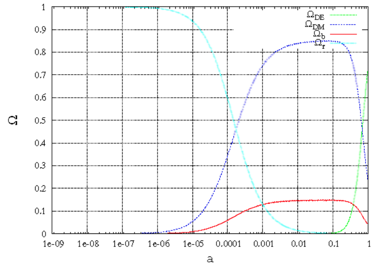

FIGURE 11. . We plot the evolution of the densities $\Omega_{\varphi_1} = \Omega_{DM}$, $\Omega_{\varphi_2} = \Omega_{DE}$, Ω_r and Ω_b. The masses are $M_2 = 1 \times 10^{-1} M_1$ and $m = 10^{-4} M_1$. The integration is made using the ABM method, integrating from $a = 1$ till $a = 10^{-9}$. The initial values for $s = 1000$, $x = 10^{-2}$ and $A = 0$.

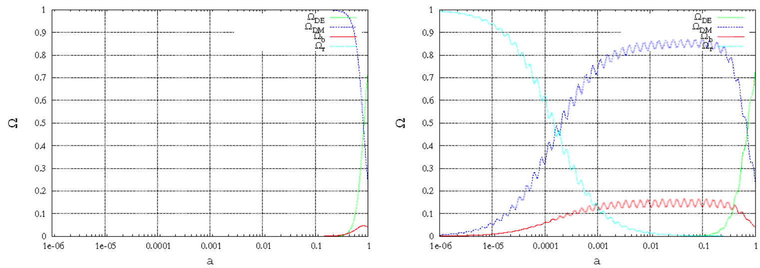

FIGURE 12. . We plot the evolutions of the densities $\Omega_{\varphi_1} = \Omega_{DM}$, $\Omega_{\varphi_2} = \Omega_{DE}$, Ω_r and Ω_b as in Fig 11. In both panels we set $m = 10^{-4}$, in the upper panel we take $M_1 = 10^{-2}$ whereas in the lower $M_2 = 10^{-1}$. The initial conditions are the same as in this figure and the integration is made using the ABM method, integrating from $a = 1$ till $a = 10^{-6}$. The initial values for $s = 1000$, $x = 10^{-5}$ and $A = 0$.

CONCLUSIONS

SFDM has provided to be an alternative model for the dark matter nature of the Universe. We have shown that the scalar field with a ultralight mass condensates very early in the Universe and generically form BEC's with a density profile which is very similar as that of the CDM model, but with a almost flat central density profile, as it seems to be in LSB and dwarf galaxies. This fact can be a crucial difference between both models. If the flat central density is no confirmed in galaxies, we can rule out the SFDM model, but if this observation is confirmed, this can be a point in favor of the SFDM model. We also show that the $1/2m^2\phi^2$ potential and the $V_0[\cosh(\kappa\lambda\phi) - 1]$ model are in fact the same. They have the same predictions, a control variable which determines the behavior of the model, given naturally the right expected cosmology and the same cosmology as the CDM model. This implies that the differences between both models, the CDM and SFDM ones, is in the non linear regime of perturbations. In this way they form galaxies and galaxy clusters, specially in the center of galaxies where the SFDM model predicts a flat density profile. If the existence of super-symmetry is confirmed, the DM super-symmetric particles would be observed by detectors and they would have the right

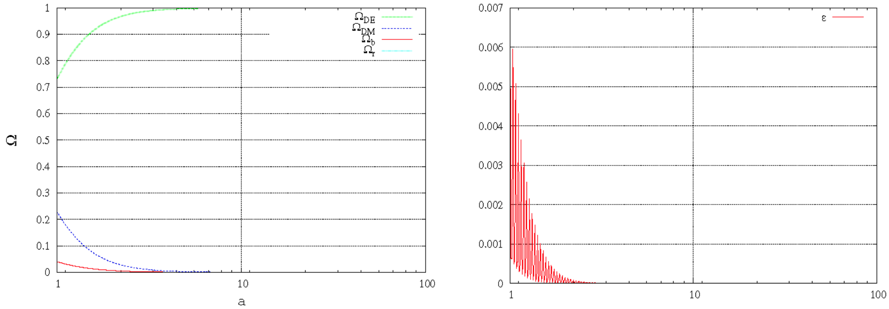

FIGURE 13. In these plots we show the evolutions of the fields (upper panel) during $N = 100$-folds. Here $m1 \times 10^{-4} M_1$ and $M_2 \sim M_1$. In the middle panel we show the evolution of the slow roll parameter ε. Observe that in this case, this parameter takes negative values. Besides, in the low panel we plot the behavior of $s \sim 1/H$, we see that this function starts in 100 and after N=100-efolds riches the value 100.045, this means that s, *i.e.* the Hubble parameter remains almost constant, indicating that the system lie in a de Sitter like behavior. Initial conditions are the same as in Fig 9.

mass, DM density and coupling constant, therefore the SFDM model can be ruled out. However, if these observations are not confirmed, the SFDM is an excellent alternative candidate to be the nature of the DM of the Universe.

ACKNOWLEDGEMENTS

We would like to thank Luis Ureña-López for his suggestions to improve the paper. Also to Blanca Moreno Ley and J. Sanchéz-Salcedo for many helpful and useful discussions. The numerical computations were carried out in the "Laboratorio de Super-Cómputo Astrofísico (LaSumA) del Cinvestav" and in the "Super-Computadora KanBalam de la UNAM". This work was partly supported by CONACyT México, under grants 49865-F, 54576-F, 56159-F, and by grant number I0101/131/07 C-234/07, Instituto Avanzado de Cosmologia (IAC) collaboration.

REFERENCES

1. Alcubierre M., Guzmán F.S., Matos T., Nuñez D., Ureña-López L.A., Wiedelhold P., 2002, Class. Quantum Grav. **19**, 5017.
2. Arbey A., Lesgourgues J., Salati P., 2003, Phys. Rev. **D 68**, 023511.
3. Arbey A., 2006, Phys. Rev. **D 74**, 043516.
4. Bernal A., Guzmán, F.S., 2006, Phys. Rev. **D 74**, 103002.
5. Bernal A., Matos T., Núñez D., 2008, RMxAA, 44, 149.
6. Bertacca D., Bartolo N., Matarrese S., 2008, JCAP **0805**, 005.
7. Cimatti et al., 2004, Nature, 430, 184.
8. Coley A.A, 1999, arXiv:gr-qc/9910074.
9. de Blok W.J.G., & Bosma A., 2002, A&A, 385, 816.
10. de Blok W.J.G., Bosma A., & McGaugh S., 2003, MNRAS, 340, 657.
11. Fukuyama T., Morikawa M., Tatekawa T., 2007, arXiv:astro-ph/0705.3091.
12. Guzmán F.S., Matos T., 2000, Class. Quantum Grav. **17**, L9.

13. Guzmán F.S., Ureña-López L. A., 2003, Phys. Rev. **D 68**, 024023.
14. Guzmán F. S., 2004, Phys. Rev. **D 69**, in press.
15. Guzmán F. S., Ureña-López L.A., 2004, Phys. Rev. **D 69**, 124033.
16. Guzmán F. S., Ureña-López L.A., 2006, ApJ, 645, 814.
17. Guzmán F. S., 2006, Phys. Rev. **D73** 021501.
18. Hinshaw G., 2008, arXiv: 0803.0732.
19. Ji S. U., Sin Sang-Jin, 1994, Phys. Rev. **D50**, 3655.
20. Lee J.W., Koh I.G., 1996, Phys. Rev. **D53**, 2236.
21. Kolb, E. W. and Turner, S. T., 1990, The Early Universe, Frontiers in Physics, Addison Wisley.
22. Lee J.W., 1996, arXiv:0801.1442.
23. Lesgourgues J., Arbey A., Salati P., 2002, New Astronomy Reviews **46**, 791.
24. Liddle A.R., Ureña-Lopez L.A., 2006, Phys. Rev. Lett. **97**, 161301.
25. Liddle A.R., Cédric P., Ureña-López L.A., 2008, arXiv:astro-ph/0804.0869.
26. Madsen J., 1992, Phys. Rev. Lett. **69**, 571.
27. Matos T., Guzmán F.S., 1999, F. Astron. Nachr. 320, 97-104.
28. Matos T., Guzmán F.S., 2000, Ann. Phys. (Leipzig), 9, SI-133.
29. Matos T., Guzmán F.S., Núñez D., 2000, Phys. Rev. **D 62**, 061301.
30. Matos T., Ureña-López L.A., 2000, Class. Quantum Grav. **17**, L75.
31. Matos T., Ureña-López L.A., 2001, Phys. Rev. **D 63**, 63506.
32. Matos T., Guzmán F.S., 2001, Class. Quantum Grav., 18, 5055.
33. Matos T., Ureña-López L.A., 2002, Phys. Lett. B **538**, 246.
34. Matos, T., Vázquez, A. & Magaña, J. A. 2008, MNRAS, **389**, in press.
35. Matos T., Ureña-López L.A., Vázquez, A. & Luebano, J. R., 2009, To be published.
36. Matos T., Vázquez, A., Pérez-Lorenzana, A., & Montesinos, M., 2009, To be published.
37. Padmanabhan T., Choudhury T. Roy, 2002, Phys. Rev. **D 66**, 081301.
38. Peebles P.J.E., Vilenkin A., 1999, Phys. Rev. **D60**, 103506.
39. Peebles P.J.E., 2000, Phys. Rev. **D62**, 023502.
40. Peebles P.J.E., 2000, ApJ, 534, L127.
41. Pérez-Lorenzana A., Montesinos M., Matos T., 2008, Phys. Rev. **D77**, 063507.
42. Press W.H., Ryden B.S., Spergel D.N., 1990, Phys. Rev. Lett. **64**, 1084.
43. Ruffini, R. and Bonazzola, S. 1969, Phys. Rev. **187**, 1767.
44. Sánchez-Salcedo F.J., Reyes-Iturbide J. & Hernandez, X., 2006, MNRAS, 370, 1829.
45. Seidel E., Suen W., 1991, Phys. Rev. Lett. **66**, 1659.
46. Seidel E., Suen W., 1994, Phys. Rev. Lett. **72**, 2516.
47. Simon J.D., Bolatto A.D., Leroy A., & Blitz L., 2005, ApJ, 621, 757.
48. Sin S.J., 1994, Phys. Rev. **D50**, 3650.
49. Turner M.S., 1983, Phys. Rev. **D 28**, 1243.
50. Ureña-López L.A., 2002, Class. Quantum Grav. **19**, 2617.
51. Ureña-López L.A., Matos T., Becerril R., 2002, Class. Quantum Grav. **19**, 6259.
52. Ureña-López L.A., Reyes-Ibarra M. J., 2007, arXiv:astro-ph/0709.3996.